



## DEVELOPMENT OF AN UPPER-BOUND METHOD FOR EXTRUSION STAMPING OF A CONICAL FLANGE

**Shokhrukh Shukhratovich Akhmadaliev**

PhD in Technical Sciences,

Tashkent State Technical University, Faculty of Mechanical  
engineering, Department of Metal technologies. 19shaxrux91@mail.ru

**Khasanov Kamoliddin Akmal ugli**

Basic Doctoral Student,

Tashkent State Technical University, Faculty of Mechanical  
engineering, Department of Metal technologies.

kamoliddinxasanov1995@gmail.com

**Saydumarov Botir Muradovich**

Associate Professor, Tashkent State Technical University, Faculty of  
Mechanical engineering, Department of Metal technologies.

botirsaydumarov@gmail.com

<https://doi.org/10.5281/zenodo.15656187>

**Annotation.** This article focuses on the application of the upper bound method for analyzing the process of extrusion stamping a conical flange. The authors emphasize that mathematical models are a key tool for optimizing complex manufacturing operations, such as extrusion, which require a deep understanding of material flows, stresses, and forces.

**Аннотация.** Данная статья посвящена применению метода верхней оценки для анализа процесса штамповки выдавливанием конического бурта. Авторы подчеркивают, что математические модели являются ключевым инструментом для оптимизации сложных производственных операций, таких как выдавливание, требующих глубокого понимания потоков материала, напряжений и сил.

**Keywords:** extrusion, upper-bound method, domain subdivision, plastic deformation zone, angular strain rates.

**Ключевые слова:** выдавливания, метод верхней оценки, разбивка, Очаг пластической деформации, угловых скоростей деформации.

The mathematical model of the extrusion process is a powerful tool for understanding and optimizing this complex manufacturing operation. Extrusion involves pushing material through a die to create a desired cross-sectional shape. Understanding the material flow, stresses, and forces involved in the process is essential for developing efficient operations and producing high-quality components.

One of the effective approaches to analyzing the extrusion process within a mathematical framework is the upper-bound method. This method provides an estimate of the power or force required for deformation, which is always greater than or equal to the actual power or force. Its main advantage lies in the fact that it does not require detailed knowledge of the internal stress distribution within the deforming material, making it simpler to apply than some other analytical techniques.

The essence of the upper-bound method is the assumption of a kinematically admissible velocity field. This means proposing a scheme of how the material flows during extrusion that satisfies the incompressibility condition and the boundary conditions (e.g., material entering and exiting the die). Once such a velocity field is defined, the internal power dissipation due to plastic deformation and friction at the die-workpiece interface can be calculated. The sum of these power dissipations gives an upper estimate of the actual power required for the

process. By minimizing this upper-bound estimate of power with respect to various parameters of the assumed velocity field, engineers and researchers can obtain a reliable estimate of the minimum required power and gain insights into optimal die designs, extrusion speeds, and lubrication conditions. This synergy between the mathematical model and the upper-bound method enables practical predictions and makes a significant contribution to the development of more efficient and cost-effective extrusion processes. In this paper, we examine the study of the extrusion process of a flange.

The main equation of the upper-bound method is given by

$$P_{\partial} = \frac{1}{v_0} \left( \sum_{m=1}^M \tau_k v_k F_k + \sum_{n=1}^N \tau_s v_c F_c \right)$$

Here,  $P_{\partial}$  is the deformation force;  $v_0$  is the tool's displacement velocity;  $M$ - is the number of contact surfaces;  $\tau_k$  is the contact shear stress;  $F_k$  is the contact surface area;  $N$ -is the number of shear surfaces;  $\tau_s$ - is the shear yield strength of the deforming material;  $v_c$ - is the relative sliding velocity of adjacent elements;  $F_c$ - is the shear surface area of adjacent elements.

This means that solving the problem using the upper-bound method involves the following procedure:

1. The deformable billet is divided into several rigid blocks to achieve the required deformation pattern through their relative motion (permissible by the tool shape).
2. Determine  $M$  and  $N$ . For each pair of adjacent blocks, find the areas of the surfaces  $F_k$  and  $F_c$ .
3. Construct the velocity hodograph for the chosen subdivision scheme. Find  $v_k$  for each contact surface and  $v_c$  for each pair of adjacent blocks.
4. Assign values to  $\tau_k$  and  $\tau_s$ .
5. Using formula (1), calculate  $P_{\partial}$ .

One of the most challenging steps in this procedure is the subdivision of the billet into blocks. This task is typically not solved by a single method. When applying the upper-bound method, several subdivision variants are considered, and the one that best captures the qualitative dependence on the main parameters and yields the absolute minimum value of  $P_{\partial}$  is selected.

As an example, consider the upsetting of a strip of unlimited length. Let the length of the strip be denoted by  $l$ , and assume  $\tau_k = \mu \cdot 2k$ .

**Variant 1.** Due to symmetry, we have

$$P_{\partial 1} = \frac{1}{v_0} 4\tau v_{2-1} F_{2-1}; \tau_s = k; v_{2-1} = \frac{v_0}{2h} \sqrt{b^2 + h^2}; F_{2-1} = \frac{1}{2} l \sqrt{b^2 + h^2} \quad (1)$$

Calculation of  $P_{\partial 1}$

$$P_{\partial 1} = kl \frac{b^2 + h^2}{h} \quad (2)$$

Calculation of  $P_{\partial 2}$ :

$$P_{\partial 2} = \frac{1}{v_0} 2[\tau_k v_{2-6} F_{2-6} + \tau_k v_{3-0} F_{3-0} + \tau_s v_{2-1} F_{2-1} + \tau_s v_{3-2} F_{3-2}]; \tau_k = \mu \cdot 2k;$$

$$v_{2-6} = v_0 \tan \alpha; F_{2-6} = \frac{bl}{2}; v_{3-0} = v_0 (\tan \alpha + \tan \beta); F_{3-0} = \left(\frac{b}{2} - h \tan \alpha\right)l;$$

$$\tau_s = k; v_{2-1} = \frac{v_0}{\cos \alpha}; F_{2-1} = \frac{hl}{\cos \alpha}; v_{3-2} = \frac{v_0}{\cos \beta}; F_{3-2} = \frac{hl}{\cos \beta}$$

Therefore,

$$P_{\partial 2} = 2kbl \left[ \mu \frac{b}{2h} + \frac{h}{b} \left( \frac{1}{\cos^2 \alpha} + \frac{1}{\cos^2 \beta} \right) \right] \quad (3)$$

Formula (1) shows that  $P_{\theta 1}$  does not depend on  $\tau_k$  (or  $\mu$ ). This is due to the way the billet is subdivided into blocks, where blocks 1 and 3 do not move relative to the dies 0 and 6 during the upsetting process.

The second variant of billet subdivision is preferable because, firstly, formula (3) expresses the qualitative dependence of  $P_\theta$  on  $\mu$ , and secondly, it results in lower values of  $P_\theta$  than the first variant (calculations performed for  $b/h=4$ ):

$\mu$	0,1	0,3	0,5
$P_{\partial 2}/P_{\partial 1}$	0,65	0,83	1,01

To obtain the optimal subdivision, Johnson and Kudo recommend first constructing an acceptable slip-line field and then replacing parts of it with other straight lines. We will demonstrate this using the example of direct extrusion. Let  $\tau_{k1} = \tau_{k3} = k$ ,  $\tau_{k2} = \tau_{k4} = 0$ .

The construction begins at point A. We draw ray AB at a  $45^\circ$  angle to the billet axis, and with radius AB we draw an arc BC. The slip-line AD is drawn such that it intersects the billet axis at a  $45^\circ$  angle. From point D, the slip-line should pass so that at point E it is tangent to the punch surface (since  $\tau_{k1} = k$ , the  $\eta$  family of lines are tangents, and the  $\zeta$  family are normals to the punch surface at point E), and at point F it intersects the die's generatrix at a  $45^\circ$  angle.

Thus, the slip-line field ABDEFCA is obtained. By straightening the arcs AD, DE, EF, FA, and AE, we obtain a subdivision of the billet into rigid triangular blocks that adequately satisfy the boundary conditions on the contact surfaces of the tool (see Fig. 1).

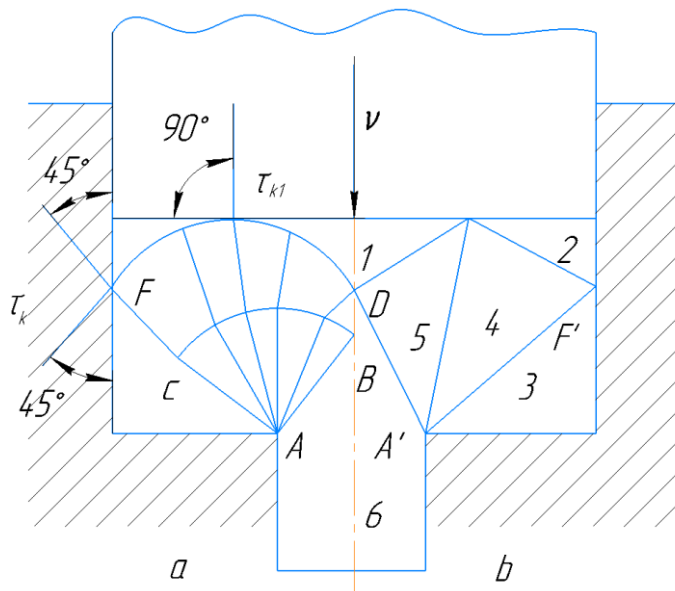


**Fig. 1. Extrusion forging of a conical flange on a rod**

As illustrated by the experience shown in Fig. 2, the extrusion stamping of a conical flange on a rod consists of two stages.

The first stage is the initiation of extrusion and the formation of the conical flange on a portion of the billet. This includes determining the specific deforming force at the initial

moment of stamping (Fig. 2a). The plastic deformation zone is concentrated in the rod at the height corresponding to the die cavity.

The second stage involves the completion of stamping and the final shaping of the flange.

**First stage:** Kinematically admissible flow velocities in the plastic deformation zone

$$v_r^* = v_0 \frac{r}{2h}$$

$$v_z^* = -v_0 \frac{z}{h} \quad (4)$$

Kinematically admissible strain rates

$$\xi_r^* = \xi_v^* = \frac{v_0}{2h}$$

$$\xi_z^* = -\frac{v_0}{2h} \quad (5)$$

Intensity of strain rates

$$\xi_i^* = v_0 \frac{1}{h} \quad (6)$$

The upper bound will be obtained after substituting expressions (4) and (6), followed by integration and transformation.

$$\frac{q}{q_s} = \sqrt{3} \left( 1 + \frac{2r}{2\sqrt{3}h} \right) = \sqrt{3} \left( \frac{r}{\sqrt{3}h} \right) \quad (7)$$

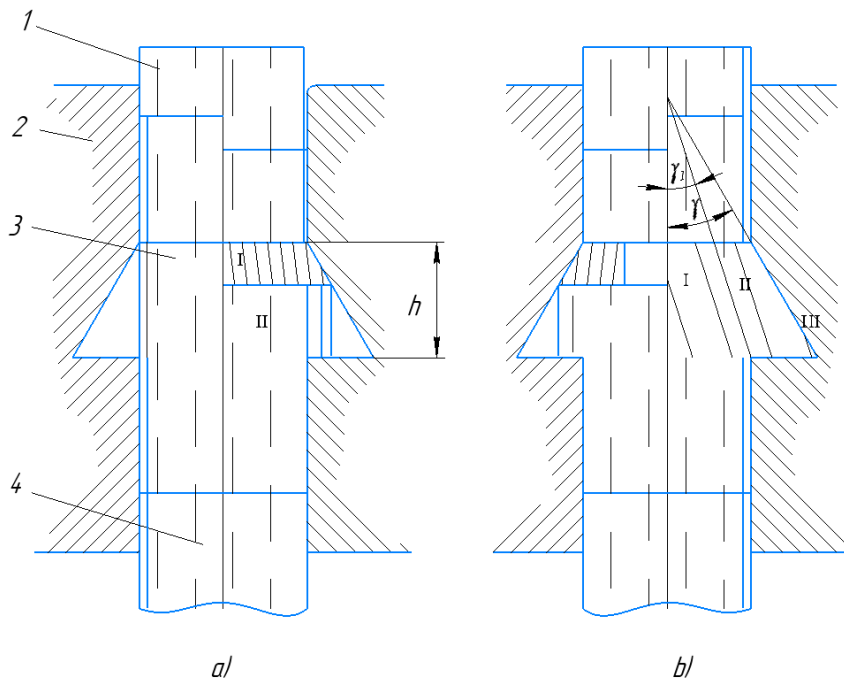


**Fig. 2. Stamping of a forging of the conical gear type**

1 – Punch; 2 – Split die; 3 – Workpiece (billet); 4 – Ejector.

A) First stage. Regions I and II of plastic deformation

B) Second stage. Regions I, II, and III of plastic deformation

The plastic deformation zone can be represented as consisting of two regions (Fig. 2).

Region I: Kinematically admissible flow velocity fields correspond to the conditions of material flow within a conical die.

$$v_r^* = v_0 \frac{r_1^2}{r^3} \cos \varphi$$

$$v_\varphi^* = v_\theta^* = 0 \quad (8)$$

Expression (8) satisfies the boundary condition  $v_r^* = \cos \varphi$  at  $r=r_1$ . In the case of radial flow at  $r=r_1$ , there is a discontinuity in the shear velocity, given by  $v_\varphi^* = -v_0 \sin \varphi$ .

Strain rate components and the intensity of angular strain rates (or angular velocity gradients

$$\xi_r^* = -v_0 \frac{r_1^2}{r^3} \cos \varphi$$

$$\xi_v^* = \xi_0^* = v_0 \frac{r_1^2}{r^3} \cos \varphi$$

$$\eta_v^* = -v_0 \frac{r_1^2}{r^3} \sin \varphi$$

$$H^* = \frac{1}{\sqrt{3}} v_0 \frac{r_1^2}{r^3} \sqrt{12 \cos^2 \varphi + \sin^2 \varphi} \quad (9)$$

In Region II, the velocity and deformation fields are described using cylindrical coordinates.

$$v_r^* = v_0 \frac{r_1^2}{R^3} \frac{r}{2h}$$

$$v_z^* = v_0 \frac{r_1^2}{R^3} \frac{z}{h} \quad (10)$$

The differential equation  $\frac{\partial v_r^*}{\partial r} + \frac{2v_r^*}{r} + \frac{v_v^* \tan \varphi}{r} + \frac{v_r^*}{r} = 0$  is solved using the method of variation of an arbitrary constant.

$$\frac{1}{r} \left( \frac{\partial v_\varphi^*}{\partial \varphi} + v_\varphi^* \tan \varphi \right) = 0 \quad (11)$$

Since in this case  $r \neq 0$  (where  $r_1 \leq r \leq R$ ), we have

$$\frac{\partial v_\varphi^*}{v_\varphi^*} = -\tan \varphi d\varphi$$

After integration,

$$\ln v_\varphi^* = c \cos \varphi \quad (12)$$

Assuming  $c=c(\varphi)$  (variation of the constant  $c$ ), the derivative is

$$\frac{\partial v_\varphi^*}{\partial \varphi} = \frac{\partial c}{\partial \varphi} \cos \varphi - c \sin \varphi$$

Substituting this expression into equation (10), we obtain:

$$-v_0 \frac{r_1^2}{R^3 - r_1^3} \left( \frac{R^3}{r^3} + 1 \right) \cos \varphi + 2v_0 \frac{r_1^2}{R^3 - r_1^3} \left( \frac{R^3}{r^3} - 1 \right) + \frac{1}{r} \left( \frac{\partial c}{\partial \varphi} \cos \varphi - c \sin \varphi + c \cos \varphi \tan \varphi \right) = 0$$

After grouping like terms and simplifying, we get:

$$v_0 \frac{r_1^2}{R^3 - r_1^3} \left( \frac{R^2}{r^2} - 3r \right) \varphi + c_1$$

By substituting  $c$  in expression (12) and determining  $c_1$  from the condition  $v_\varphi^* = 0$  at  $\varphi = 0$ , we obtain:

$$v_\varphi^* = -v_0 \frac{r_1^2}{R^3 - r_1^3} \left( \frac{R^3}{r^2} - 3r \right) \varphi \cos \varphi \quad (13)$$

The intensity of angular strain rates is:

$$H^* = \frac{2}{3} v_0 \frac{r_1^2 \cos \varphi}{R^3 - r_1^3} \sqrt{\frac{R^6}{r^6} + 3 + \frac{1}{4} \left[ \varphi - \left( \frac{R^3}{r^2} - 1 \right) \tan \varphi \right]} \quad (14)$$

**Region III:**

In this region, the flow is assumed to be radial. To satisfy the continuity condition at  $\varphi = \gamma_1$  (the boundary between Regions II and III), the boundary conditions are relaxed so that the flow rates in Regions II and III are equal.

Thus, the flow  $Q$  through the boundary surface at  $\varphi = \gamma_1$  for Region II is:

$$Q|_{\varphi=\gamma} = \int_{r_1}^R v_{\varphi}^*|_{\varphi=\gamma} 2\pi r \sin \gamma_1 dr = -\pi v_0 \frac{r_1^2}{R^3-r_1^3} \gamma_1 (\sin 2\gamma_1) \left[ R^3 \left( \ln \frac{R}{r_1} - 1 \right) + r_1^3 \right] \quad (3.49)$$

Then,

$$v_{\varphi}^*|_{\varphi=\gamma} = \frac{Q \sin \gamma_1}{\pi(R^2-r_1^2)} = -\frac{v_0 r_1^2 \gamma_1 \sin 2\gamma_1 \sin \gamma_1}{(R^3-r_1^3)(R^2-r_1^2)} \cdot \left[ R^3 \left( \ln \frac{R}{r_1} - 3 \right) + r_1^3 \right] \quad (15)$$

Considering the boundary condition (15) for radial flow,  $v_r^* = \frac{A}{r^2}$  we solve the differential equation based on the volume constancy condition (similarly to Region II), and obtain:

$$v_{\varphi}^* = \frac{v_0 r_1^2 \gamma_1^3 \sin 2\gamma_1 \sin \gamma_1}{(R^3-r_1^3)(R^2-r_1^2)(\gamma^2-\gamma_1^2)} \left[ R^3 \left( 3 - \ln \frac{R}{r_1} \right) - r_1^3 \right] \left[ \left( \frac{\gamma^2}{\varphi} - \varphi \right) \right]$$

$$v_r^* = v_{\varphi}^* = \frac{v_0 r_1^2 \gamma_1^3 \sin 2\gamma_1 \sin \gamma_1}{(R^3-r_1^3)(R^2-r_1^2)(\gamma^2-\gamma_1^2)} \left[ R^3 \left( 3 - \ln \frac{R}{r_1} \right) - r_1^3 \right] \left[ \left( \frac{\gamma^2}{\varphi} - \varphi \right) \tan \varphi - \frac{\gamma^2}{\varphi^2} - 1 \right] \left( \frac{r_1^2}{r^2} - 1 \right) + v_0 \frac{r_1^2}{r^2} \cos \varphi \quad (16)$$

Expressions (16) allow determining the kinematically admissible strain rates and the intensity of angular strain rates, and ultimately the upper bound estimate of the deforming force.

The performed calculations are in agreement with the data from experimental studies.

## References:

1. Abdullaev, F., Ismailov, X., Akhmadaliev, S., & Khasanov, K. (2021). Determination of Force Factors During Precipitation. International Journal on Orange Technologies, 3(3), 261-264.
2. Abdullayev, F. S., Khasanov, K. A., & Abdullayev, R. F. (2021, December). PIKABUR BODY DETAIL AND STAMP PROJECT FOR ITS PRODUCTION. In Здравствуйте, уважаемые участники международной научной и научно-технической конференции, дорогие гости! (p. 307).
3. Абдуллаев, Ф. С. (2000). Махкамов Қ. Металларга босим билан ишлов бериш назарияси асослари. Ўқув қўлланма. Тошкент: ТДТУ.
4. Ахмадалиев, Ш. Ш., Загидуллин, Р. Р., & Усмонжонов, С. И. (2021, December). БУРҒУЛАШ ИШЛАРИДА ҚЎЛЛАНИЛАДИГАН “ПИКАБУР” НИ ОЛИШДАГИ ЭКСПЕРИМЕНТАЛ УСКУНА. In Здравствуйте, уважаемые участники международной научной и научно-технической конференции, дорогие гости! (p. 295).
5. Мохов А.И., Кобелев А.Г., Троиский В.П. Оборудование-кузнечно-штамповочных сехов: В 2 ч. Ч. 1. Прессы: Учеб. для вузов. – Волгоград: Изд-во ВолГТУ, 2000. – 410 с.
6. Liu HS, Xing ZW, Bao J and Song BY, Investigation of the Hot-stamping Process for Advanced High-strength Steel Sheet by Numerical Simulation, Journal of Materials Engineering and Performance, 2010, 19(3), 325-334
7. Hu P, He B and Ying L, Numerical Investigation on Cooling Performance of Hot Stamping Tool with Various Channel Designs, Applied Thermal Engineering, 2016, 96, 338-351.
8. Caron E, Daun KJ and Wells MA, Experimental Characterization of Heat Transfer Coefficients during Hot Forming Die Quenching of Boron Steel, Metallurgical and Materials Transactions B, 2013, 44(2), 332-43.